LIMNOLOGY
and
OCEANOGRAPHY

ASLO

Limnol. Oceanogr. 61, 2016, 1916–1931

doi: 10.1002/lno.10347

Intertidal salt marshes as an important source of inorganic carbon to the coastal ocean

Zhaohui Aleck Wang,*[1] Kevin D. Kroeger,[2] Neil K. Ganju,[2] Meagan Eagle Gonneea,[2] Sophie N. Chu[1]
[1]Department of Marine Chemistry and Geochemistry, Woods Hole Oceanographic Institution, Woods Hole, Massachusetts
[2]Woods Hole Coastal and Marine Science Center, United States Geological Survey, Woods Hole, Massachusetts

Abstract

Dynamic tidal export of dissolved inorganic carbon (DIC) to the coastal ocean from highly productive intertidal marshes and its effects on seawater carbonate chemistry are thoroughly evaluated. The study uses a comprehensive approach by combining tidal water sampling of CO_2 parameters across seasons, continuous in situ measurements of biogeochemically-relevant parameters and water fluxes, with high-resolution modeling in an intertidal salt marsh of the U.S. northeast region. Salt marshes can acidify and alkalize tidal water by injecting CO_2 (DIC) and total alkalinity (TA). DIC and TA generation may also be decoupled due to differential effects of marsh aerobic and anaerobic respiration on DIC and TA. As marsh DIC is added to tidal water, the buffering capacity first decreases to a minimum and then increases quickly. Large additions of marsh DIC can result in higher buffering capacity in ebbing tide than incoming tide. Alkalization of tidal water, which mostly occurs in the summer due to anaerobic respiration, can further modify buffering capacity. Marsh exports of DIC and alkalinity may have complex implications for the future, more acidified ocean. Marsh DIC export exhibits high variability over tidal and seasonal cycles, which is modulated by both marsh DIC generation and by water fluxes. The marsh DIC export of 414 g C m^{-2} yr^{-1}, based on high-resolution measurements and modeling, is more than twice the previous estimates. It is a major term in the marsh carbon budget and translates to one of the largest carbon fluxes along the U.S. East Coast.

The land-sea interface is a biogeochemical hotspot where estuaries, coastal wetlands, and the adjacent coastal ocean are interwoven. Biogeochemical processes, exchanges, and fluxes of carbon at or across this interface are important to the carbon cycle, and thus have influential feedbacks to global climate (Mackenzie et al. 2004; Hales et al. 2008; Liu et al. 2010; Cai 2011). However, coastal systems are inherently challenging to study due to their highly heterogeneous nature in time and space, and current assessments of carbon fluxes across this interface still have large uncertainties (Seitzinger et al. 2005; Chen and Borges 2009; Cai 2011; Najjar et al. 2012; Bauer et al. 2013; Herrmann et al. 2015).

*Correspondence: zawang@whoi.edu

Additional Supporting Information may be found in the online version of this article.

Carbon assimilation in vegetated coastal systems, such as intertidal salt marshes, is among the highest in the biosphere, with Gross Primary Production (GPP) ranging from 1900 g C m^{-2} yr^{-1} to 3600 g C m^{-2} yr^{-1} and Net Ecosystem Production from 150 g C m^{-1} yr^{-1} to 1600 g C m^{-1} yr^{-1} (Hopkinson 1988; Duarte et al. 2005; Hopkinson and Smith 2005; Gedan et al. 2009). It has long been recognized that coastal salt marshes "outwell" organic carbon (OC) and nutrients via tidal exchange (Odum 1968; Childers et al. 2000), though the effect of such export on estuarine and coastal marine ecosystems remains poorly resolved. Globally, vegetated coastal systems export OC at 0.2–0.3 Pg C yr^{-1} (Duarte et al. 2005; Cai 2011; Bauer et al. 2013), a carbon source that may fuel the net heterotrophy of the coastal ocean (Smith and Hollibaugh 1993; Mackenzie et al. 2004).

Only more recently, studies have shown that various respiration processes in marsh sediments also result in the increase of dissolved inorganic carbon (DIC) concentration and partial pressure of CO_2 (pCO_2) in tidal water. Subsequently, added DIC is "outwelled" to coastal water by tidal exchange or emitted as CO_2 to the atmosphere (Morris and Whiting 1986; Kumar et al. 1993; Cai and Wang 1998; Raymond et al. 2000; Raymond and

Hopkinson 2003; Wang and Cai 2004). A "Marsh CO_2 Pump" concept was proposed to conceptualize tidal marshes as a net atmospheric CO_2 sink and a source of inorganic carbon to the coastal ocean (Wang and Cai 2004), although flux estimates are available from only a handful of studies. Based on a study conducted in Duplin River, a marsh-dominated tidal creek on Sapelo Island, GA, the salt marsh exports DIC on the order of 156 g C m^{-2} yr^{-1} (Wang and Cai 2004). This rate is comparable to the estimate of the salt marsh DIC export in South Carolina (Capone et al. 1983; Morris and Whiting 1986) and in Virginia freshwater marshes (Neubauer and Anderson 2003). These estimates were based on discrete sampling events at monthly to seasonal intervals, with a sampling resolution from hourly to one half of a tidal cycle, leaving the majority of time unsampled, and thus requiring large interpolation between sampling events. DIC export flux was estimated based on the volume of the tidal prism and DIC concentrations. However, such sampling strategies have been shown to produce substantial uncertainty in export fluxes (Downing et al. 2009; Ganju et al. 2012). It is thus reasonable to argue that previous studies may not fully resolve the export magnitude and temporal heterogeneity, which may be controlled by variability in both water flux and constituent concentration across time scales from minutes to tidal cycles to seasons.

Tidal water, after exchange with salt marshes, may also contain higher total alkalinity (TA), indicating that marshes also export TA (Wang and Cai 2004). Anaerobic respiration in marsh sediments generates most of the exported alkalinity (Giblin and Howarth 1984; Giblin and Wieder 1992; Raymond and Hopkinson 2003). Sulfate reduction is often a major remineralization pathway, resulting in pyrite burial that is long removed from the contemporary biogeochemical cycle (Howarth 1979; Howarth and Merkel 1984; Giblin 1988). Marsh TA export could be an important term in the overall coastal ocean alkalinity budget (Thomas et al. 2009; Hu and Cai 2011). Interestingly, in addition to higher alkalinity, ebbing tide also has much lower pH than flooding tide (Wang and Cai 2004; Jiang et al. 2008). This reveals an apparent paradox, where the effects of tidal exchange with marshes are both acidifying and alkalizing coastal waters. This aspect of tidal exchange with salt marshes must be fully resolved to determine if and how marsh DIC and TA exports influence the buffering capacity of the coastal ocean. This is particularly relevant to potential future changes in seawater chemistry under ongoing anthropogenic pressures such as coastal ocean acidification, and world-wide loss of coastal wetlands due to sea level rise and other factors.

In this article, we analyze the role of intertidal salt marshes in altering carbonate chemistry and buffering capacity of tidally-exchanged water over various temporal scales from an intertidal salt marsh in the U.S. northeast temperate region. To resolve the high temporal variability of tidal carbon fluxes from marshes, readily available in-situ sensors were deployed to make high-frequency measurements of both biogeochemically relevant parameters and tidal water fluxes. Those data were combined with DIC bottle measurements to empirically model DIC concentration and derive DIC fluxes over tidal to annual scales. Such a strategy may have broad applicability to resolve lateral transport of chemical species from similarly dynamic environments. This study is the first to obtain realistic, highly dynamic DIC concentration and fluxes during the exchange between tidal marshes and coastal water and thus vastly improves the assessment of lateral DIC export fluxes from intertidal salt marshes. We further examined the implications of the new flux estimate to the coastal carbon budget along the U.S. East Coast.

Methods

Study site and drainage area

The study site, Sage Lot Pond (SLP), is an intertidal salt marsh near the eastern inlet of Waquoit Bay (Fig. 1), an estuary on the south coast of Cape Cod, Massachusetts (MA), United States. It is part of the Waquoit Bay National Estuarine Research Reserve (WBNERR). The salt marsh at SLP shares many similarities with other Atlantic salt marshes, including floral (high marsh dominated by *Distichlis spicata* and *Juncus gerardii*, low marsh dominated by *Spartina alterniflora* with minor occurrence of *S. patens*) and faunal communities, relative sea level rise (2.83 ± 0.18 mm yr^{-1}, NOAA Tide Station ID 8447930; www.tidesandcurrents.noaa.gov), and mean annual temperature (9.8°C) is close to the average (8.2°C) for 58 study sites along the east coast of U.S. and Canada (Chmura et al. 2003). This is important with regard to examining the implications of our results across a larger scale and in comparison to other important coastal carbon fluxes. The marsh peat overlies a sandy coastal aquifer and reaches a maximum thickness of 3 m at the marsh edge. A small marsh creek within SLP was selected for this study to produce a relatively well-constrained tidal flooding and drainage basin area, water budget, and area-normalized constituent flux estimates. The groundwater input to the drainage area is relatively insignificant with an annual flux of 6310 m^3 estimated based on the isohaline method of MacCready (2011) and salt balance as applied by Ganju (2011). SLP has a small, forested watershed with relatively low nutrient load (12 kg N ha^{-1} yr^{-1}) (Kroeger et al. 2006). The environmental setting of SLP is thus ideal for a fundamental baseline study.

To measure tidal exchange of inorganic carbon within the SLP marsh, a time-series sampling site was established at the mouth of a tidal creek that drains a portion of the marsh (Fig. 1). Both high-frequency sensor measurements and discrete sampling were obtained at this site. To evaluate export of DIC from the study marsh on a unit area basis, the marsh drainage area of the tidal creek was defined using a water routing analysis in the Global Mapper program. A 1-m bare-earth LiDAR-derived digital elevation model (DEM) of Massachusetts based on the North American Vertical Datum of 1988 (NAVD88) (http://catalog.data.gov/dataset/2011-u-s-geological-survey-topographic-lidar-lidar-for-the-north-east) was used along with a

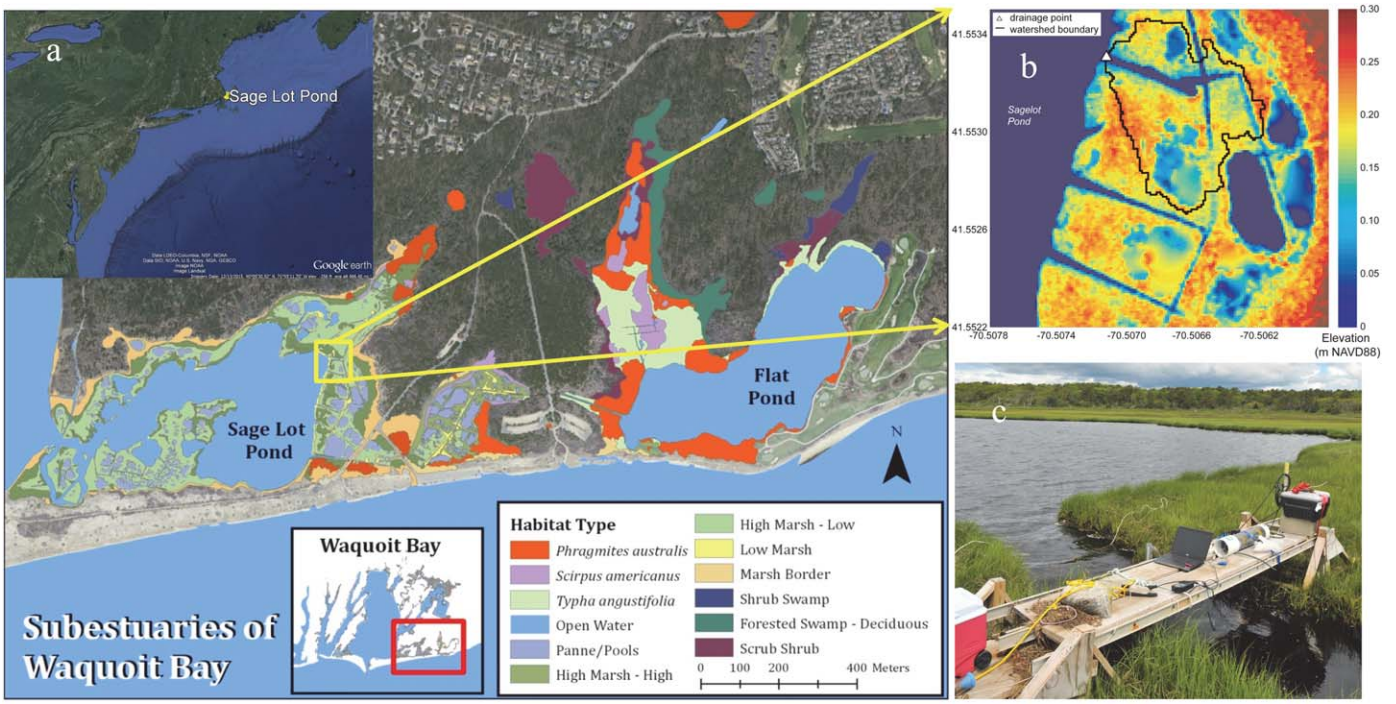

Fig. 1. Study site and sampling location. **(a)** Area map of Waquoit Bay and Sage Lot Pond (courtesy of Jordan Mora of WBNERR); **(b)** Elevation (color) and marsh drainage basin (black line) of the sampled tidal creek. Triangle, the creek mouth sampling site (drainage point); **(c)** The sampling bridge at the creek mouth sampling site.

water-drop analysis routine to route water from the marsh surface to the creek mouth sampling site (Fig. 1). The landward ponds were excluded due to a topographic high that prevents exchange between the ponds and the creek except at the highest tides. The area of the watershed was computed as 4132 m^2.

Sampling and measurements

High-resolution, time-series measurements of biogeochemical and physical parameters were made from November 2012 to November 2014 at the tidal creek sampling site (Fig. 1) using in-situ sensors. Sensors included a Sontek IQ Plus acoustic Doppler current profiler (ADCP) for measurements of water flux and water surface elevation, and a YSI EXO2 Sonde for salinity (S), temperature (t), water depth, dissolved oxygen, oxidation-reduction potential (ORP), pH, fluorescence of dissolved organic matter (FDOM), and turbidity. The YSI EXO2 recorded measurements at intervals ranging from 2 min to 8 min and the Sontek IQ recorded time-averaged data every 15 min. The relative elevation of the deployed Sontek IQ was referenced to NAVD88, which is based on repeated long-term GPS base station occupations using a Trimble receiver (±3 cm). Error associated with relative elevation is negligible. All sensors were physically cleaned, calibrated, and maintained at regular intervals using manufacturer recommended methods to maintain performance. After a deployment period of typically 2–4 weeks, performance of YSI Sonde was evaluated for fouling and calibration drift using calibration standards. Based on post-deployment calibration, a correction factor was applied linearly to the data (i.e., no correction at the beginning of the deployment, full correction at the end); when such correction was >30% of the calibration value (ORP and salinity) or >2 pH units (pH), all of which were larger than observed natural variability, that data was discarded (Wagner et al. 2006).

EXO2 pH measurements (NBS scale) have a measurement uncertainty of ± 0.10 pH units. EXO2 pH data were only used for DIC modeling. All other measurement uncertainties can be found at https://www.ysi.com/EXO2. The water fluxes in and out of the creek are internally calculated by the Sontek IQ proprietary software, which employs the user-provided cross-sectional geometry of the creek, measured velocities, and water depth to estimate water flux. The uncertainty in water flux arising from velocity measurement as well as the internal algorithms is less than 3.7% (http://www.sontek.com/productsdetail.php?SonTek-IQ-Series-15).

Hourly discrete bottle samples of carbonate parameters (DIC and TA) were obtained at the tidal creek sampling site using a peristaltic or diaphragm pump over full tidal cycles in April, July, and November 2012, and June, July, August, and October 2013. Discrete samples were collected following the best practice of seawater CO_2 measurements outlined in Dickson et al. (2007). Briefly, water samples for DIC and TA

were pumped through 0.45 μm capsule filters (Farrwest Environmental Supply, Texas, USA) and collected into 250 (or 500) mL borosilicate glass bottles. Each sample was poisoned with 100 (or 200) μL mercuric chloride, and sealed with glass stoppers coated with APIEZON®-L grease and fixed with rubber band on the top.

To gauge DIC input from groundwater discharge, groundwater DIC samples were also collected from the sandy coastal aquifer immediately upland of the salt marsh in September 2014, and April, July, and October 2015 using a MHE Push-Point™ sampler. Water was pumped from depths ranging between 0.5 m and 2.0 m below the land surface into a syringe through a 0.22 μm filter to reduce microbial activities. Then, 3 mL of water were injected into a sealed and helium flushed 5 mL glass vial pre-capped with a crimped, butyl septum, immediately stored on ice and frozen within 12 h.

Discrete DIC samples of tidal water were measured by a DIC auto-analyzer (AS-C3, Apollo SciTech Inc., Delaware, USA), in which each sample was acidified with 10% phosphoric acid, and subsequently purged of total CO_2 with nitrogen gas. The gas stream was then detected by a LiCOR7000 infrared CO_2 analyzer (LI-COR Environmental, Nebraska, USA). The instrument was calibrated with Certified Reference Material (CRM) from Dr. A.G. Dickson at the Scripps Institution of Oceanography. A modified Gran titration procedure (Wang and Cai 2004; Wang et al. 2013) was used to determine TA with hydrochloric acid (HCl) on an automated titrator (AS-ALK2, Apollo SciTech Inc., Delaware, USA) using an open-cell configuration and a ROSS™ combination electrode at 22.0 ± 0.1°C. HCl was calibrated using CRMs. DIC and TA values were reported in μmol kg^{-1} after being corrected for water density and mercuric chloride addition. Both DIC and TA measurements had a precision and accuracy of ± 2.0 μmol kg^{-1}. Discrete pH in total scale (pH_T) was calculated using bottle DIC and TA data with the CO_2 program by Pierrot et al. (2006). Carbonic acid dissolution constants of Millero et al. (2006) were used for the calculation.

Groundwater DIC samples (Supporting Information Table S1) were measured with a CO_2 coulometer (UIC Inc., Illinois, USA) following the procedure by Dickson et al. (2007). After acidification in the sealed vial with 85% phosphoric acid, CO_2 was stripped from the samples with a helium carrier gas and adsorbed by an ethanolamine solution, followed by photometrically monitored titration using thymolphthalein as the indicator. The CRMs were used as a reference standard to calibrate the system. The CRMs were prepared and measured in the same manner as samples to evaluate the uncertainty of groundwater DIC measurements due to sampling, storage, and analysis. The results show an overall uncertainty of ~2%.

Buffer factors

Various buffer factors can be used to quantify changes in seawater buffering capacity during the tidal exchange with the marsh. They are a measure of the resistance of seawater to a given chemical perturbation, such as addition of acid or CO_2. In this study, pH related buffer factor β_H and Revelle Factor (R) related buffer factor γ_{DIC} (Morel and Hering 1993; Egleston et al. 2010) are used for discussion. They are defined as:

$$\beta_H = -\left(\frac{\partial pH}{\partial [H^+]}\right)^{-1} \quad (1)$$

$$\gamma_{DIC} = -\left(\frac{\partial \ln [CO_2]}{\partial [DIC]}\right)^{-1} = DIC/R \quad (2)$$

β_H is a traditional measure of buffering capacity and quantifies how much pH would change for a given addition of acid or base, while γ_{DIC} is inversely related to R and describes how much aqueous CO_2 would change for a given change in DIC concentration. β_H and γ_{DIC} follow similar change patterns for a given change of seawater chemistry, such as ocean acidification (Egleston et al. 2010). Both of these factors were calculated using measured DIC, TA, salinity, and temperature data based on the equations derived by Egleston et al. (2010). Unknown non-carbonate alkalinity, if present in a significant quantity, may affect these calculations. Based on nutrient data, phosphate and silicate alkalinity are negligible (<4 μmol kg^{-1}) for this study. Direct titration of non-carbonate alkalinity of selected bottle samples (Cai and Wang 1998) collected from tidal cycles indicate that other unknown alkalinity, presumably mostly organic alkalinity, vary from negligible in flooding tidal water to ~100 μmol kg^{-1} in ebbing water from the marsh during the seasonal sampling events. The composition, quantity, and chemical properties (e.g., dissociation constants) of chemical species contributing to organic alkalinity are required to quantify the effect of organic alkalinity on the calculation of buffer factors. However, the effect should be mostly minor for buffer factor calculation, since unknown alkalinity has been included in the TA measurements (total titration alkalinity) and they also contribute buffering capacity. In the above calculation (Eqs. 1, 2), organic alkalinity was treated as part of carbonate alkalinity. In the most extreme case of summer, when organic alkalinity can reach ~100 μmol kg^{-1} in ebbing tide with DIC ~ 2600 μmol kg^{-1}, TA ~ 2100 μmol kg^{-1}, S ~ 28, t = 25°C (mean condition of the ebbing tide in summer), and if the organic acid has a pK of ~5.4 (Cai and Wang 1998), the calculation only underestimates β_H and γ_{DIC} on the order of < 10%.

DIC model

A DIC concentration model based on a multi-linear regression (MLR) analysis was developed using discrete DIC bottle measurements and sensor measurements to derive high-frequency DIC concentrations. Modeled DIC data were then combined with high-frequency water fluxes to quantify instantaneous DIC fluxes between the marsh and coast

during the study period. The initial independent variables include time of the year (Julian Day) and sensor (EXO2 YSI Sonde) measured parameters (S, temperature, water elevation, pH, O_2, FDOM, and ORP). The final variables of the model were selected based on their physical or biogeochemical relevance with DIC concentrations, the strength of their statistical association, and their data quality and availability among other statistical principles:

$$\mathrm{DIC}\ (\mu\mathrm{mol\ kg^{-1}}) = k + a(\mathrm{Day}') + b(S) + c(\mathrm{pH}) + d(\mathrm{ORP}) \quad (1)$$

where $\mathrm{Day}' = \cos\left(\frac{2\pi(JDay-\gamma)}{365}\right)$, and JDay is Julian day.

The Day′ term represents the seasonal changes of marsh DIC generation caused by respiration processes. This seasonality is associated with the marsh life cycle (see later discussion). Day′ was calculated by transforming Julian day (JDay, 1 d - 365 d) sinusoidally. Such a transformation allows January to be close to February and December so that they are treated as winter months (Lefevre et al. 2005; Friedrich and Oschlies 2009). γ is a phase parameter that was optimized by varying it between 0 and 365 to achieve a minimum root-mean-square-error. A similar MLR approach has been used in recent coastal CO_2 studies (Hales et al. 2012; Signorini et al. 2013). S reflects effects of mixing on DIC variability. ORP and pH are indicators of the influence of marsh respiration processes on water chemistry, as both aerobic and anaerobic respiration generate DIC that is subsequently exported via tidal exchange. The details of the model are shown in Supporting Information (Supporting Information Text S1, Fig. S1). The model is able to capture ~74% of the DIC variability without systematic errors, and has a standard error of estimate of 131 μmol kg^{-1}. Such an error has limited effects on final DIC flux estimates because: (1) the model error is random so that the integration of instantaneous DIC fluxes with opposing directions (signs) over tidal cycles results in the errors canceling out; (2) DIC variability over tidal and seasonal cycles is often much larger than the model error (see details in *"Lateral DIC flux from salt marshes"* in Results and Discussion).

Water fluxes

The within-creek, high-resolution water fluxes gauged by the ADCP measurements (Q_b) were treated as the baseline data to derive the water fluxes used for calculation of high-resolution DIC fluxes. We performed two corrections to Q_b to account for two other water flux contributions to the marsh. The corrected high-resolution water fluxes (Q_t) can be written as: $Q_t = f_o Q_b + \bar{Q_w}$. The positive flow direction is to the marsh. The first term is to amplify Q_b by a factor f_o to account for overland flow not measured by the within-creek ADCP. Overland flow occurs if flooding or ebbing tidal water inundates the marsh without going through the creek channel when tidal height is above the marsh surface. Factor f_o is the ratio of total (to and from the drainage area) to within-channel water fluxes. It is a function of water level and flow direction (Supporting Information Fig. S2, Text S2). The second term is to shift the time-series of flow by 0.0007 $m^3\ s^{-1}$ ($\bar{Q_w}$) so that the mean flow over the entire study period matched the net groundwater estimate (−0.0002 $m^3\ s^{-1}$ or −6310 $m^3\ yr^{-1}$). $\bar{Q_w}$ is only 0.3% of the mean tidal flow magnitude (0.075 $m^3\ s^{-1}$).

If overland flow is unaccounted for, it may lead to a flood or ebb bias in the water fluxes depending on how the portion of the total fluxes within the channel during flooding tides compared to that during ebbing tides. It may also result in an underestimation of peak fluxes in and out of the drainage area. To estimate overland flow contribution (f_o) to Q_t, we developed a hydrodynamic model in the drainage basin of the tidal creek for the marsh plain up to the upland boundary using the 1-m DEM with the Coupled Ocean-Atmosphere-Wave-Sediment Transport (COAWST) model (Warner et al. 2010) (Supporting Information Text S2, Fig. S2). The results indicate that during peak flooding, on average ~50% of the water occurred as overland flow, and that the channel-based measurement is ebb-biased (Supporting Information Text S2).

Results and discussion

Variability of carbonate chemistry in marsh tidal water

Changes of carbonate chemistry in tidal water due to exchange with marshes reflects two distinct drivers: the seasonal progression of biological activity primarily in the marsh, and hydrodynamic forcing that "outwells" DIC, alkalinity, and hydrogen ions (H^+) via tidal exchange, producing patterns of mixing between coastal and marsh endmembers. Seawater DIC is the sum of all inorganic carbon species, including aqueous CO_2, bicarbonate (HCO_3^-), and carbonate (CO_3^{2-}) ions, while total alkalinity is mostly comprised of HCO_3^-, CO_3^{2-}, and borate, with other weak base species, such as organic alkalinity, contributing significantly in special cases. In addition, the same biogeochemical process may affect DIC and TA differently, and variability of DIC and TA can be decoupled at certain times of the year (Fig. 2). In spring (April), both DIC and TA show relatively small variability over a tidal cycle, and concentration gradients between high tide water (largely reflecting the coastal endmember) and low tide water (reflecting the marsh-influenced endmember) were small; pH varied from ~7.5 at the low tide to ~8.1 at the high tide; pCO_2 showed the opposite trend to pH (data not shown). These data indicate that the marsh processes generate CO_2 and hydrogen ions (H^+) even this early in the growth season. DIC values were generally less than TA, a typical condition of seawater where CO_3^{2-} provides the first line of buffering capacity. However, at low tide DIC concentrations slightly increased, and were similar to TA (Fig. 2), indicating that most of the CO_3^{2-} may be converted to HCO_3^- via addition of CO_2 through marsh

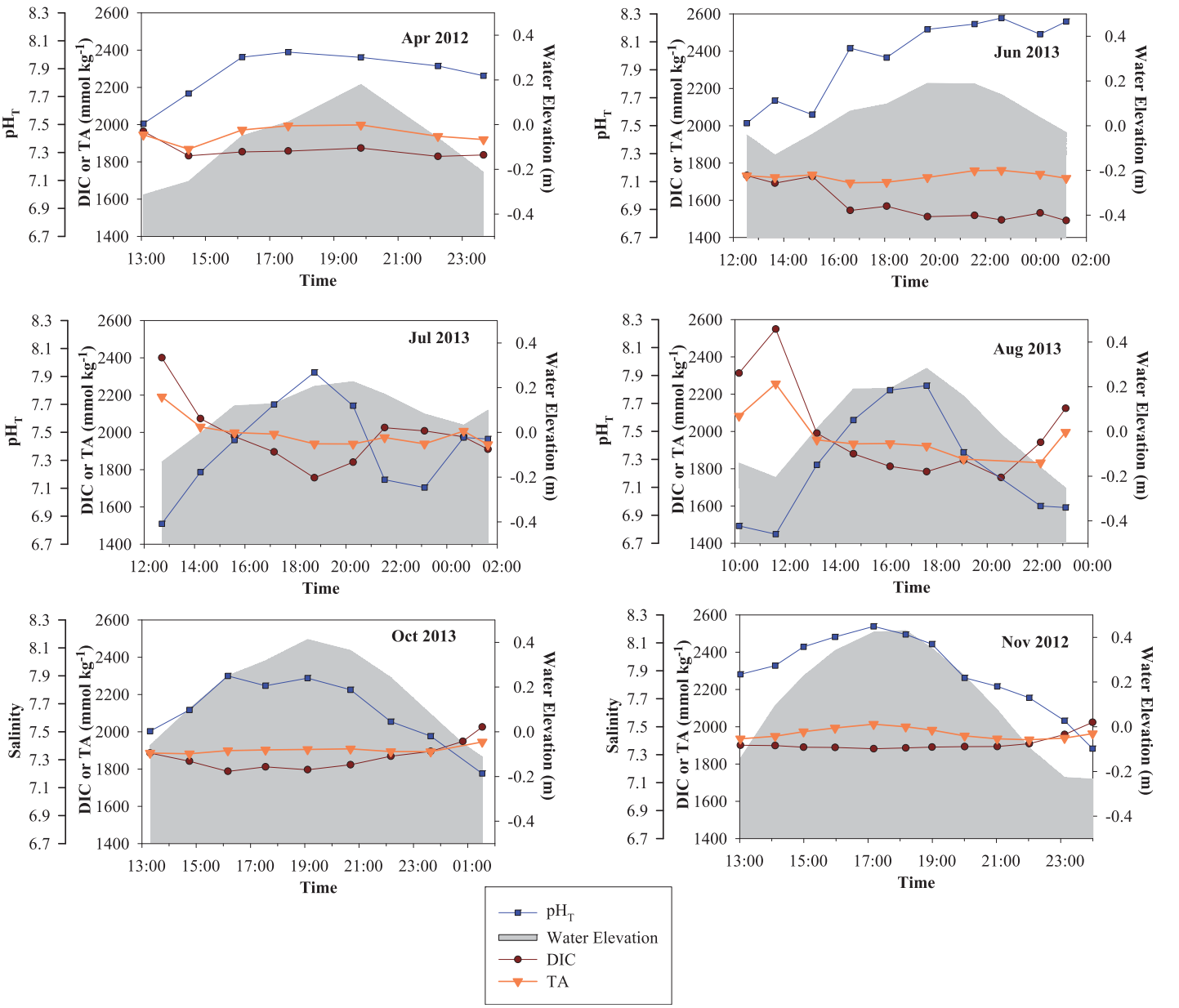

Fig. 2. Tidal time-series evolution of water elevation, DIC, TA, and pH_T at the Sage Lot Pond over different seasons. The plots are organized to progress through the seasons from spring to fall and each parameter uses the same scale for comparison. Data from July 2012, which were similar to those from July 2013, were not shown. See salinity data in Supporting Information Fig. S3.

respiration. In spring, production of DIC and H^+ seemed to be solely supported by aerobic respiration in the marsh, as TA varied little between high and low tide.

In early summer (June), there was a clear divergence between DIC and TA over the tidal cycle, where TA stayed relatively stable, as was observed in the spring, while DIC showed a clear increase from high to low tides (Fig. 2). Again, TA was higher than DIC except during low tide, and aerobic respiration appeared to be dominant. pH and pCO_2 showed patterns similar to those in April. In summer (July and August), the magnitude of DIC increase from high to low tides was much higher than June. TA also showed a similar trend, but the increase was lower in magnitude than that of DIC. Summer pH and pCO_2 showed larger variation over a tidal cycle than June and April. Increase of TA from high to low tides indicates generation of alkalinity in the marsh via anaerobic respiration (Giblin et al. 1990; Giblin and Wieder 1992; Wang and Cai 2004). Anaerobic respiration, such as sulfate (SO_4^{2-}) reduction and denitrification, produces a net gain of HCO_3^-, and thus a net addition of alkalinity, if there are external sources of electron donors (e.g., SO_4^{2-} and NO_3^-) for these processes to occur (Hu and Cai 2011). Over a tidal cycle,

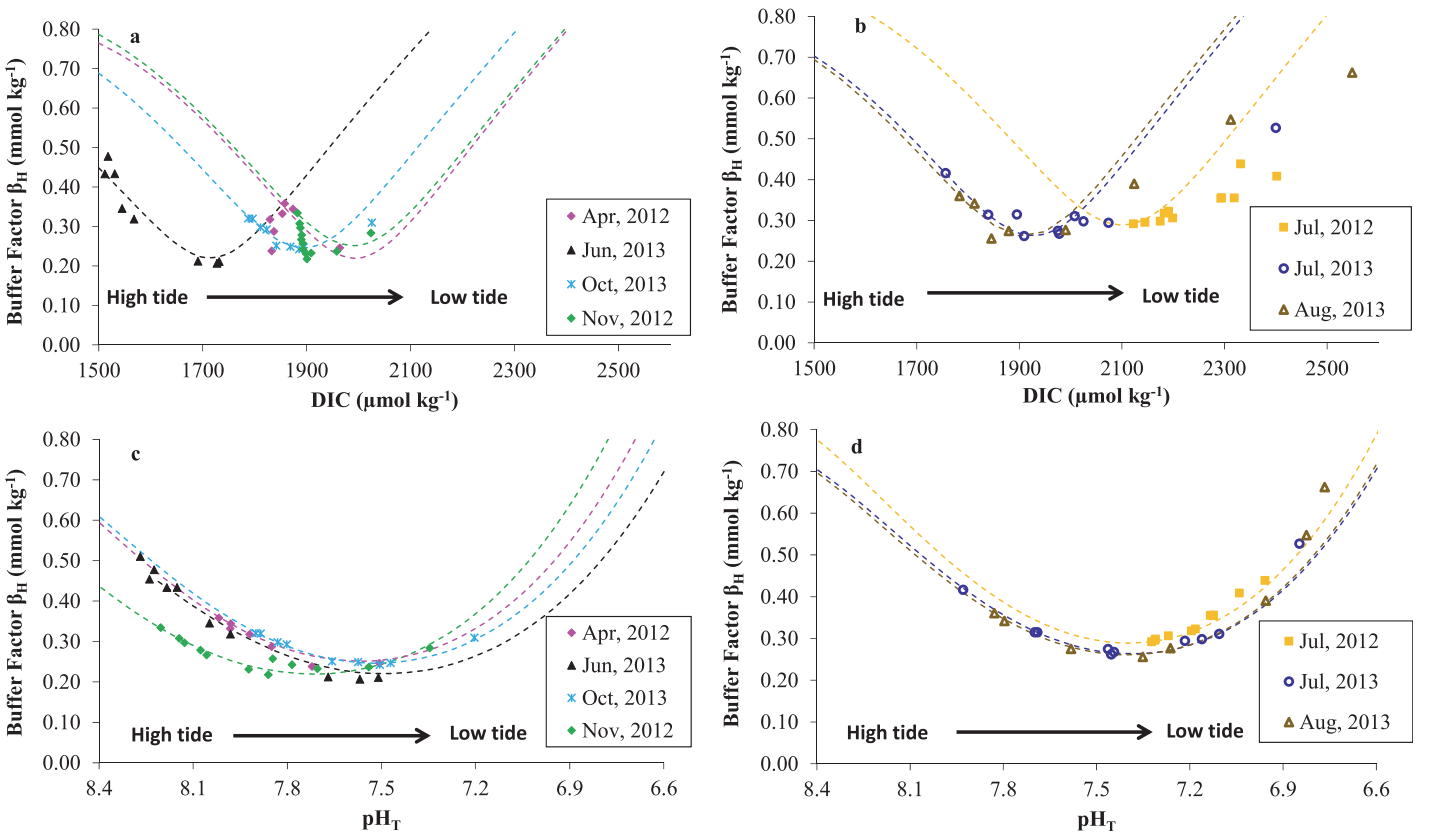

Fig. 3. Buffer factor β_H as a function of DIC (**a** and **b**) and pH$_T$ (**c** and **d**) over tidal cycles at different seasons. Note that pH$_T$ was calculated from DIC and TA and its scales in c and d are in reverse order, progressing from left to right (high to low values). Colored dashed lines are theoretical contour lines of β_H vs. DIC or pH at a fixed TA; they match the data in color for each sampling event. The contour lines are calculated using high tide (coastal endmember) TA with varying DIC, mean temperature, and salinity of each seasonal sampling event, representing how the buffering capacity of incoming tidal water would change during the course of interaction with the marsh if only DIC is added to tidal water.

there is a larger addition of DIC than TA to tidal water, since both aerobic and anaerobic respiration generate DIC in the marsh, while only anaerobic respiration generates TA (Fig. 2). Different from June and April, except at high tide, DIC concentration surpassed TA most of the time over a tidal cycle. This indicates that during the marsh tidal exchange, all the CO_3^{2-} in seawater has been titrated by the large addition of CO_2 (DIC) from marsh respiration processes, such that carbonate species in the tidal water leaving the marsh mostly consists of HCO_3^- and aqueous CO_2.

In October and November, DIC and TA variations over a tidal cycle were similar to June, although pH in the ebbing tide remained at levels similar to those observed in summer (Fig. 2). Both DIC and H^+ were still being generated in fall in the marsh, while there was no clear production of alkalinity. These measurements indicate that both aerobic and anaerobic respiration processes in the marsh likely slowed down with cooler temperatures in fall.

Paradox of acidification and alkalization

Production of DIC, H^+, and alkalinity, decoupling between DIC and TA, and their seasonal variabilities in the SLP marsh are similar to those observed in salt marshes of the U.S. southeast region (Wang and Cai 2004), although even higher concentration gradients and longer generation seasons were observed there. An interesting and seemingly paradoxical aspect of those findings is that marsh processes can acidify and alkalize coastal water during the period (e.g., summer) when there are net gains of both DIC (with associated H^+) and alkalinity over a tidal cycle (Fig. 2). Similar to marshes, it has been suggested that coastal sediments may provide significant buffering capacity to coastal oceans by exporting alkalinity (Thomas et al. 2009). However, the observation shown here indicates that alkalinity and DIC generation in marshes are decoupled. With greater DIC production than TA occurring for a longer portion of the annual cycle, DIC generation plays the primary role of influencing tidal water buffering capacity, while TA release from the marsh exerts a relatively small effect.

Such a phenomenon was demonstrated by variations of buffering capacity over tidal cycles at different seasons (Fig. 3), which reveal how seawater interaction with the marsh profoundly changes water carbonate chemistry and modifies

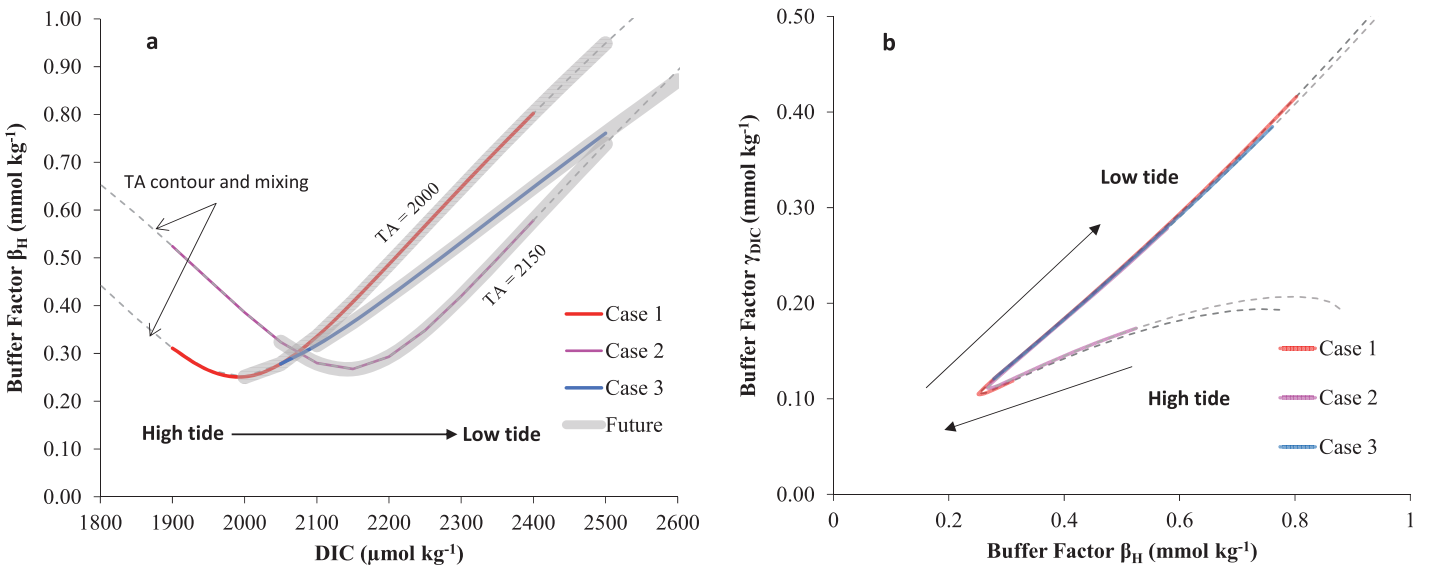

Fig. 4. (a) Theoretical curves of buffer factor β_H as a function of DIC for three cases. Broken dash lines are TA contour lines. Case 1 (red line), DIC addition (1900–2600 μmol kg^{-1}), TA = 2000 μmol kg^{-1}; Case 2 (pink line), DIC addition (1900–2600 μmol kg^{-1}), TA = 2150 μmol kg^{-1}; Case 3 (blue line), DIC and TA addition, with the increase of TA from 2000 μmol kg^{-1} to 2150 μmol kg^{-1} and DIC from 2050 μmol kg^{-1} to 2600 μmol kg^{-1}. For all cases, the mean salinity (S = 26.2) and temperature (t = 17.8°C) of all sampling events in Sage Lot Pond were used for calculation. The three future scenarios (thick gray lines) corresponding to the three cases were calculated by assuming pCO_2 in respective incoming tidal water increases at the same rate as in the atmosphere to the end of the century (+ 400 μatm) without TA change. **(b)** The relationship of β_H and γ_{DIC}. Cases and lines are the same as in (a).

buffering capacity by adding DIC (and H^+) alone or adding DIC and alkalinity together. It is noted that alkalinity reflects the acid neutralizing capacity relative to pH ~4.5 not necessarily an indicator of buffering capacity.

Changes in buffer factor β_H over tidal and seasonal cycles (Fig. 3) are in concert with marsh addition of DIC (and H^+) and TA to tidal water (Fig. 2). The TA contour lines in Fig. 3 represent how the buffering capacity of incoming tidal water at each sampling event would change during the course of interaction with the marsh if only DIC is added to tidal water. In spring (April), the change in β_H was relatively small over a tidal cycle and did not follow the TA contour lines clearly (Fig. 3a,c). However, by early summer (June), coastal DIC was relatively low, and as the tide fell, the increase in DIC, along with pH decrease, resulted in a β_H decrease from 0.15 at high tide to near the minimum at low tide (Fig. 3a,c). Such a change closely followed the theoretical TA contour lines of DIC addition. This is consistent with the observation in June that the marsh only injected a small amount of CO_2 (DIC) into tidal water, but no net gain of TA (Fig. 2). The result was a decrease in seawater buffering capacity upon tidal exchange with the marsh. The buffering capacity reaches a minimum when DIC ~ TA and the pH of seawater is about half way between carbonic acid pK_1 and pK_2 (K_1 and K_2 are the first and second dissocation constants of carbonic acid) at a given condition. This is consistent with the traditional knowledge that the buffering capacity of a weak acid solution is at maximum when the pH is close to the pKa of the weak acid, and it decreases as pH moves away from the pKa (Morel and Hering 1993).

In summer (July and August), a much larger addition of DIC by the marsh pushed buffering capacity in tidal water beyond the minimum point and into the region of the TA contour lines where buffering capacity increases with increasing DIC concentration. As a result, ebbing tidal water had substantially higher buffering capacity than flooding water (Fig. 3b,d). Moreover, addition of alkalinity from anaerobic respiration causes β_H to vary between the theoretical TA contour lines over the tidal cycle (Fig. 3b,d). In October, β_H mostly varied along the TA contour lines, but with much less range over a tidal cycle. By November, variations of DIC concentration and β_H over a tidal cycle were small (Fig. 3a), and β_H still varied in a large pH range somewhat along the TA contour line (Fig. 3c). However, β_H at low tide in October and November still passed through the β_H minimum. It is interesting to note that in the summer, low pH water in ebbing tide can have a higher buffering capacity than high pH water in flooding tide (Fig. 3d). This means that the tidal water draining out of the marsh (with lower pH) is more resistant to pH change for a given addition of acid (e.g., CO_2) than the coastal water (with higher pH).

The relationship between β_H, DIC, and pH observed during tidal exchange with the marsh can be reasonably described by three theoretical cases (Fig. 4a), which demonstrate how interactions with the marsh can modulate carbonate chemistry in tidal water. Cases 1 and 2 both

represent the situation where only DIC is added to tidal water by marsh aerobic respiration, but under low (Case 1) and high (Case 2) initial TA conditions in incoming coastal water. They mostly illustrate the early summer and fall conditions in SLP, although DIC addition via marsh tidal exchange was relatively small (Fig. 3a,c). Change in TA during aerobic respiration is insignificant and thus is ignored in this analysis. Case 3 represents the summer condition where both DIC and TA are added via tidal exchange with the marsh as a result of both aerobic and anaerobic respiration. Typical incoming coastal water before tidal exchange with the marsh contains <10% of its DIC as CO_3^{2-}. Addition of DIC (CO_2) to this water via aerobic respiration will titrate CO_3^{2-} to HCO_3^- and thus buffering capacity will initially decrease. When all of the CO_3^{2-} is titrated, buffering capacity reaches a minimum with TA ≈ DIC. If DIC continues to be added, β_H will begin to increase (Fig. 4a) and buffering capacity is mostly provided by HCO_3^- after the β_H minimum. During this process, H^+ always increases (or pH decreases) regardless of buffering capacity changes, as pH change is dominated by inputs of CO_2 (Fig. 3c,d). Depending on the initial conditions of tidal water, the net effects on buffering capacity by marsh aerobic respiration can be different. In Case 1 where the buffer factor of the incoming tide is close to its minimum, addition of DIC by exchange with marsh will quickly push β_H past the minimum and cause it to increase quickly afterwards. Case 2 has relatively high buffering capacity initially in coastal water such that a significant amount of DIC increase leads to lower buffering capacity at the beginning until β_H passes its minimum. Cases 1 and 2 are similar to ocean acidification, as the input of CO_2 is the main driver for changes of buffering capacity.

In Case 3, a large amount of DIC and TA are both added to tidal water during exchange with the marsh due to aerobic and anaerobic respiration, as observed in summer (Fig. 3). As a result β_H passes its minimum, and increases afterwards; at the same time β_H also shift from a lower to a higher TA contour line (Figs. 3, 4). The net result is that β_H in ebbing tides is substantially higher than that in flooding tides. pH changes in Case 3 depend on both increases of DIC and TA. A similar conclusion can be reached if buffer factor γ_{DIC} is used since β_H and γ_{DIC} covary almost linearly (Fig. 4b). Interestingly, this covariation follows a lower slope before the buffer factor minimum than after it. In other words, as CO_2 is added to the seawater, the rate at which β_H and γ_{DIC} decrease is slower towards each of their respective minimums than the rate at which they increase after the minimum. It should be noted that because the acidification process (CO_2 addition) during the tidal exchange may cause γ_{DIC} to pass its minimum and result in higher γ_{DIC}, or lower Revelle Factor (R) (Eq. 2), the traditional way of interpreting R (and γ_{DIC}), where lower R means higher CO_2 uptake capacity, may no longer apply here. On the contrary, water pCO_2 always increases during exchange with the marsh, so that the resulting water has higher CO_2 degassing potential. However, consistent with the γ_{DIC} definition, seawater with higher γ_{DIC} means its aqueous CO_2 concentration would change less than that with lower γ_{DIC} for a given change in DIC.

It is clear from this analysis that increases of acidity, alkalinity, and buffering capacity can occur during the exchange with the marsh over the same tidal cycle, and their variability can be reasonably modeled based on theoretical CO_2 calculation and knowledge of aerobic and anaerobic respiration in the marsh. The net effects of tidal exchange on the buffering capacity of coastal water depend on initial conditions and the amount of DIC and TA addition. Essentially, the differences in DIC and TA generation between aerobic and anaerobic respiration and their variability cause both the observed decoupling of variation in DIC and TA and the relationship between β_H, DIC, and pH in tidal water exchanging with marshes over tidal and seasonal scales. This study demonstrates that tidal marshes may play an important role in regulating the buffering capacity of coastal water over a long time scale, similar to rivers.

Such a conclusion may have long-term and complex implications to a more acidified coastal ocean in the future. As ocean acidification continues, the buffering capacity of the coastal water flooding into marshes will continue to decrease (Fig. 4). By the end of this century, the buffer factor of coastal water could be potentially near its minimum. As such, DIC addition via tidal exchange with marshes would elevate buffering capacity of tidal water to a greater extent than it does currently (Fig. 4). However, the implication of such a change on the chemical resistance of the future coastal ocean may be multi-dimensional. For example, on the one hand, the same amount of marsh DIC exports in the future may acidify coastal water further than they do today (Fig. 4a). On the other hand, because this export may further elevate β_H, coastal water would have more chemical resistance against other pH changes than today. What this means for the biology and ecology of the coastal ocean is unknown. Further studies regarding this topic are thus necessary.

Lateral DIC flux from salt marshes

The net effects of tidal exchange between the marsh and coastal ocean on the buffering capacity rely in large part on the magnitude of DIC export flux. Below, we constrain DIC export from the salt marsh, as well as factors controlling temporal variability in flux. Ultimately, we demonstrate that DIC flux is an important component of the carbon budget within the marsh and in the coastal ocean.

DIC flux sensitivity and correction

High-frequency DIC concentration and fluxes derived from modeling allow evaluation of the sensitivity of marsh DIC fluxes to uncertainties in the DIC model and water fluxes. We applied 100 realizations of random errors simultaneously to the discrete data of the independent variables

Table 1. Monthly and annual DIC fluxes (g C m^{-2} marsh yr^{-1}). Negative sign indicates export from the marsh to the coast.

	DIC base fluxes*	DIC fluxes with overland flow correction	DIC fluxes with overland flow and GW flow correction	%Data coverage‡
Apr	−331	−17	−138	48
May	−644	−266	−385	40
Jun	−1455	−382	−501	64
Jul	−1368	−391	−516	37
Aug	−1478	−425	−556	53
Sep	−1281	−511	−645	58
Oct	−650	−153	−285	21
Nov	−946	−385	−518	37
Dec	−928	−251	−376	44
Mean	−1053	−323	−450	45
Annual DIC Flux, Marsh Source†			−414	

*The base fluxes are total net DIC flux in the creek, calculated by multiplying modeled DIC concentration with instantaneous water fluxes. Monthly fluxes were calculated by averaging all instantaneous fluxes in a given month during a two-year period (November 2012 to November 2014).
†Annual marsh flux was calculated by deducting GW DIC flux (−36 g yr^{-1} m^{-2}marsh) from the calculated annual mean; Jan–Mar were not included in annual flux calculation (see text for details).
‡%Data coverage is the percentage of the time that had instantaneous DIC flux data for a given month over the two-year period.

used to derive the MLR DIC model (Eq. 1), with a maximum error margin of 10% of the observed values except pH, which was constrained to an error of ± 0.1 pH units. These uncertainties are all greater than or similar to analytical errors of individual measurements. The MLR procedure was repeated for the DIC model, and DIC fluxes recalculated each time. The mean base DIC flux (Table 1) of all realizations was 996 g C m^{-2} yr^{-1} with a standard deviation of 15 g C m^{-2} yr^{-1}. Separately, we simultaneously applied a 10% error (and ± 0.1 for pH) to all high-resolution data of independent variables (high-frequency sensor data plus Day′) used to calculate fluxes, resulting in a standard deviation of < 1 g C m^{-2} yr^{-1} in the mean DIC flux. A similar sensitivity was conducted to water fluxes with a random error of 3.7%, the maximum error of velocity measurements. The resulting DIC flux had an error of less than 1%. As such, the DIC flux is relatively insensitive to random errors of DIC concentration, the parameters used in the DIC model, and water fluxes. This is mostly because random errors in the parameters used to calculate DIC fluxes would cause random errors in fluxes with opposite direction, thus cancelling out in the net flux. If combining the maximum measurement uncertainties for all parameters used in DIC flux estimates, i.e., 5% for S and ORP, 0.1 for pH, 3.7% for water fluxes, and assuming 5% for Day′, the overall uncertainty in DIC fluxes can be approximated as 9.5% based on the method using individual errors (Ganju et al. 2005).

As a result of overland flow correction (See Methods), the monthly and annual mean seaward DIC fluxes were all reduced significantly from the base fluxes (Table 1). After both overland and groundwater (GW) flow corrections (Table 1), the results reflected the total DIC fluxes that include DIC generated by marsh respiration and GW DIC input. GW discharge has two mechanisms to contribute to DIC export fluxes. The first is that GW can cause a net seaward flow of water, simply acting as a carrier (without DIC concentration) to flush out more marsh DIC; the second is to directly discharge DIC since it has DIC content derived from terrestrial sources. In this study, the first mechanism was still treated as DIC export from the marsh as flushed carbon is still marsh carbon; the second mechanism, direct DIC input from GW, was removed to derive the annual mean DIC flux from the marsh (Table 1). Although GW DIC concentration was only measured seasonally and is not able to be modeled in high-resolution to correct instantaneous DIC fluxes for direct GW DIC inputs, its annual mean estimate (36 ± 7 g C m^{-2} yr^{-1}; with uncertainty reflecting the overall uncertainty in GW DIC measurements) is only about 8.6% of annual mean DIC flux (414 g C m^{-2} yr^{-1}, Table 1), suggesting its contribution to DIC fluxes on tidal to seasonal scales is likely minor at this site.

Variability of DIC fluxes

Mean monthly DIC fluxes show that the marsh exports DIC between April and December (negative fluxes; Fig. 5), with the maximum rates occurring in August–September. The DIC fluxes from January to March were excluded from monthly and annual flux calculations due to three reasons. First, the marsh was frozen most of time in January, February, and March, thus DIC production and exchange should be at a minimum. Second, there were no collections of bottle DIC samples from January to March. Third, corresponding data coverage from sensor measurements was limited. The

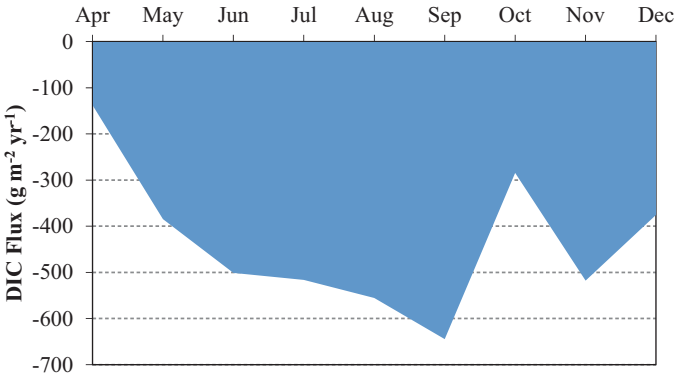

Fig. 5. Mean monthly DIC fluxes at the Sage Lot Pond, Cape Cod, MA. Data from Table 1.

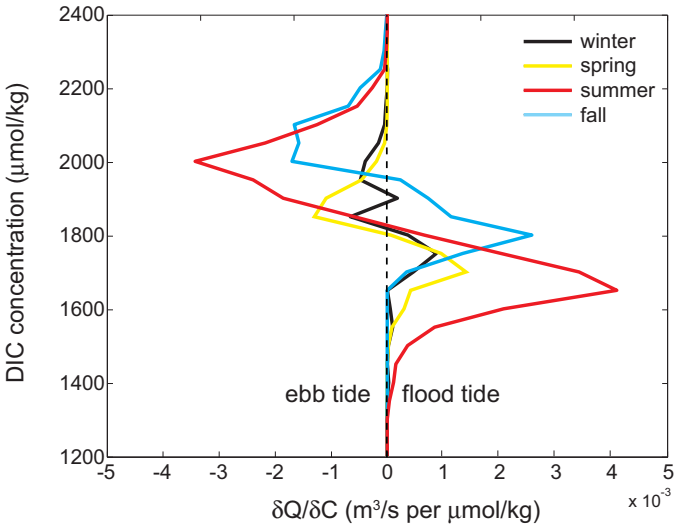

Fig. 6. Seasonal modeled DIC concentration as a function of net tidal water fluxes for a given binned DIC concentration ($\delta Q/\delta DIC$). Modeled DIC concentrations are binned over four seasons (December–February, March–April, May–July, September–November). The net tidal water fluxes in a given DIC concentration bin ($\delta Q/\delta DIC$) were calculated by summing all instantaneous water fluxes in that bin.

annual mean DIC flux from our calculation thus represents a flux during the nine non-winter months, and thus is likely a conservative annual estimate.

As with the discrete sampling events discussed above, the model data, which covers a much wider range of physical and tidal conditions in the marsh, further demonstrates that water acquires DIC upon tidal exchange and that this process varies seasonally (Fig. 6). Following the differential isohaline transport concept (MacCready 2011), net water transport within DIC concentration space demonstrates the acquisition of DIC following tidal exchange. The calculation of net water transport in this sense negates water fluxes of the same concentration entering or exiting the channel, therefore small water transport values ($\delta Q/\delta C$) indicate minimal transformation of water masses for a given DIC bin, not minimal water flux. In spring, both DIC concentration and net water transport per unit DIC were low, resulting in small net seaward transport of DIC from the marsh. Maximum DIC transformation from high to low tide and high DIC concentration in ebb tide in summer produced the maximum DIC export rates from the marsh. Although the ebb tide still has relatively high DIC concentration in the fall, the net DIC export rate is smaller than that in summer because the transformation of water from high to low tide is less. In winter, limited data suggest that both DIC concentration and transformation were at the annual minima, resulting in insignificant seaward DIC fluxes.

The seasonal pattern of the DIC flux at SLP (Figs. 5, 6) is similar to that in previous studies of salt marshes (Wang and Cai 2004) and tidal freshwater marshes (Raymond et al. 2000; Neubauer and Anderson 2003) along the U.S. southeast coast. Such seasonality at least partially reflects the growth-senescence cycle of marsh plants. Net growth in marshes occurs at a high rate in spring and the respiration rate is relatively low, corresponding to relatively small DIC export. In summer, higher temperatures and more available marsh carbon stock fuel high rates of both aerobic and anaerobic respiration, corresponding to high rates of DIC export. Finally, in fall and continuing into winter, a decrease in temperature slows respiration and DIC export despite ongoing availability of marsh carbon sources; low temperatures should correspond to minimum DIC export in winter.

However, one of the main differences between this and previous studies is that the DIC fluxes are significantly higher. The annual mean areal DIC export flux from the SLP marsh is more than twice the rates reported by Wang and Cai (2004) and Neubauer and Anderson (2003). Both of these previous studies generally showed larger DIC gradients between high and low tides than those observed at SLP (Fig. 2). Their study sites in general also have higher temperature to promote greater respiration rates and longer growth seasons. Indeed, their marsh DIC export rates were relatively high throughout summer and fall, while at SLP, the export has already slowed down in fall (Fig. 5). As such, the main reason for much higher rates of DIC export in the SLP may be due to capturing concentration changes and water fluxes at much higher resolution. For example, Wang and Cai (2004) and Neubauer and Anderson (2003) use high-low tide DIC gradients and tidal prism volumes to estimate DIC fluxes. However, instantaneous water flux plays an important role in shaping the instantaneous DIC fluxes, as the two tracked closely with each other most of the time (e.g., Supporting Information Fig. S4). Indeed, the largest instantaneous water and corresponding DIC fluxes occur near the high tide right before and after the tidal flow turns direction. Thus, the majority of DIC flux occurs during only a portion of tidal exchange near high tide when water fluxes are

greatest both into (flood) and out of (ebb) the marsh. In addition, the previous studies did not capture the large—up to 10-fold—differences in DIC fluxes between spring and neap tidal cycles (Supporting Information Fig. S4). The new estimates of DIC export from marshes thus demonstrate not only the magnitude of the flux, but also for the first time, the details of how and when DIC transformation and transport occur over tidal cycles in a realistic and dynamic way.

Significance to the coastal carbon budget

More high-resolution studies across different marsh sites with different characteristics are needed to examine if previous assessments of marsh DIC export are indeed significantly underestimated, as demonstrated in this study, and to accurately quantify DIC fluxes from marshes on a larger scale. It is noted that all current large scale estimates of marsh inorganic carbon fluxes are only based on 3–4 previous studies (Cai 2011; Bauer et al. 2013) with the methodological limitations discussed above. Herein we scaled up the new annual areal DIC export from the marsh (414 g C yr^{-1} m^{-2}) to the U.S East Coast (Fig. 7a) to examine its potential significance in the context of the regional carbon budget. The justification is that such an exercise might be a relatively conservative estimate due to several reasons: (1) DIC concentrations measured in tidal water of the SLP marsh in the U.S. northeast region are relatively low compared to those south of the study site (Raymond et al. 2000; Neubauer and Anderson 2003; Wang and Cai 2004). (2) The water fluxes at SLP should be in the range of other marsh sites, given that the maximum tidal range here is about 1 m and GW discharge is low. In addition, the new estimates resolve the DIC export from marshes on a more realistic temporal scale (tidal to seasonal cycles), and are thus more robust than previous estimates used to derive the marsh carbon budget in the U.S. East Coast (Cai 2011; Kroeger et al. 2012). This scale-up can be viewed as an initial attempt to examine the implication of the new estimate to the U.S. East Coast carbon budget and to help generate future hypotheses and questions, not to provide a definitive regional flux estimate.

This scale-up exercise indicates that tidal marshes along the U.S. East (Atlantic) Coast export 5.1 Tg C yr^{-1} as DIC (1 Tg = 10^{12} g) to the coastal ocean (Fig. 7a). This is larger than either riverine DOC (3.9 Tg C yr^{-1}) or DIC (3.0 Tg C yr^{-1}) flux (Najjar et al. 2012), and is about twice of the annual shelf CO_2 sink. The new marsh DIC flux is a factor of 3 greater than either the marsh burial rate (blue carbon) or the DOC export flux. It is comparable to the modeled cross-shelf DIC flux. As such, the tidal marsh DIC export is among the largest carbon fluxes along the U.S. East Coast and its impact on the coastal carbon budget and carbon cycling is potentially greater than previously reported. Given the magnitude of marsh DIC export, and its potential to significantly modify seawater buffering capacity (Figs. 3, 4), such an export may also be an important factor that determines the chemical resistance of coastal water along the East Coast over a long term.

Recent synthesis studies of the coastal carbon cycle (Cai 2011; Bauer et al. 2013) suggest that globally, tidal wetlands export DIC at a rate either lower than or similar to the DOC rate. However, the results of this study suggest marsh DIC export flux may have been significantly underestimated. It has been noted that up to 50% of the net primary production of global mangroves, another type of tidal wetland, is exported as DIC to the coastal ocean based on a mass balance of all synthesized carbon fluxes for mangroves (Bouillon et al. 2008). Herein, a scale-up exercise was also conducted to examine the potential significance of the new marsh DIC export rate to the tidal marsh carbon budget for the U.S. East Coast. Direct assessments of DIC exports from tidal marshes are still rare, with this study being the first to achieve such high temporal resolution across the most time of a year, thus a synthesis on the topic is still preliminary. Nevertheless, the goal here is not to close the marsh carbon budget or provide a synthesis, but rather to provide evidence that marsh DIC export flux is likely a primary term in the marsh carbon cycle. A bottom-up method was used to identify all available carbon fluxes in tidal marshes and compare the sum of them to measured net primary production (NPP) in marshes. Other sources of carbon fluxes, such as groundwater and riverine inputs, are not considered in this exercise for simplicity. These carbon sources are either lacking or insignificant for our study site.

In this scale-up exercise, except the areal marsh DIC flux obtained from this study, all other marsh carbon fluxes and East Coast marsh area were adopted from literature reviews (Fig. 7b). The terms of these marsh carbon fluxes mimic those presented by Bouillon et al. (2008) and Cai (2011). The CO_2 evasion flux includes CO_2 degassing from both marsh sediments and tidal water inundating marshes, accounting for 4.4 Tg C yr^{-1} or more than 1/3 of the tidal marsh NPP (Fig. 7b). The DIC export represents about 5.1 Tg C yr^{-1} or 39% of the marsh NPP. This is followed by the DOC export (~12%) and carbon burial (or blue carbon; ~11%). The POC export (~5% of NPP) is less than one half of the DOC flux or carbon burial. The budget suggests that the majority (>70% of NPP) of fixed carbon by marsh plants is either returned to the atmosphere or exported to the coastal ocean as inorganic carbon (CO_2 gas and DIC). Notably, the DIC export flux is more than three times of the DOC flux, which is almost the opposite of the recent synthesis of the coastal carbon cycle (Bauer et al. 2013). However, the DIC flux from this study aligns with that exported from global mangroves (Bouillon et al. 2008), where DIC export is more than twice of the DOC export. All available tidal marsh data (Cai 2011; Kroeger et al. 2012) indicate that changes of DIC concentration over tidal cycles across all seasons are almost always higher than changes of DOC concentration. For any given site,

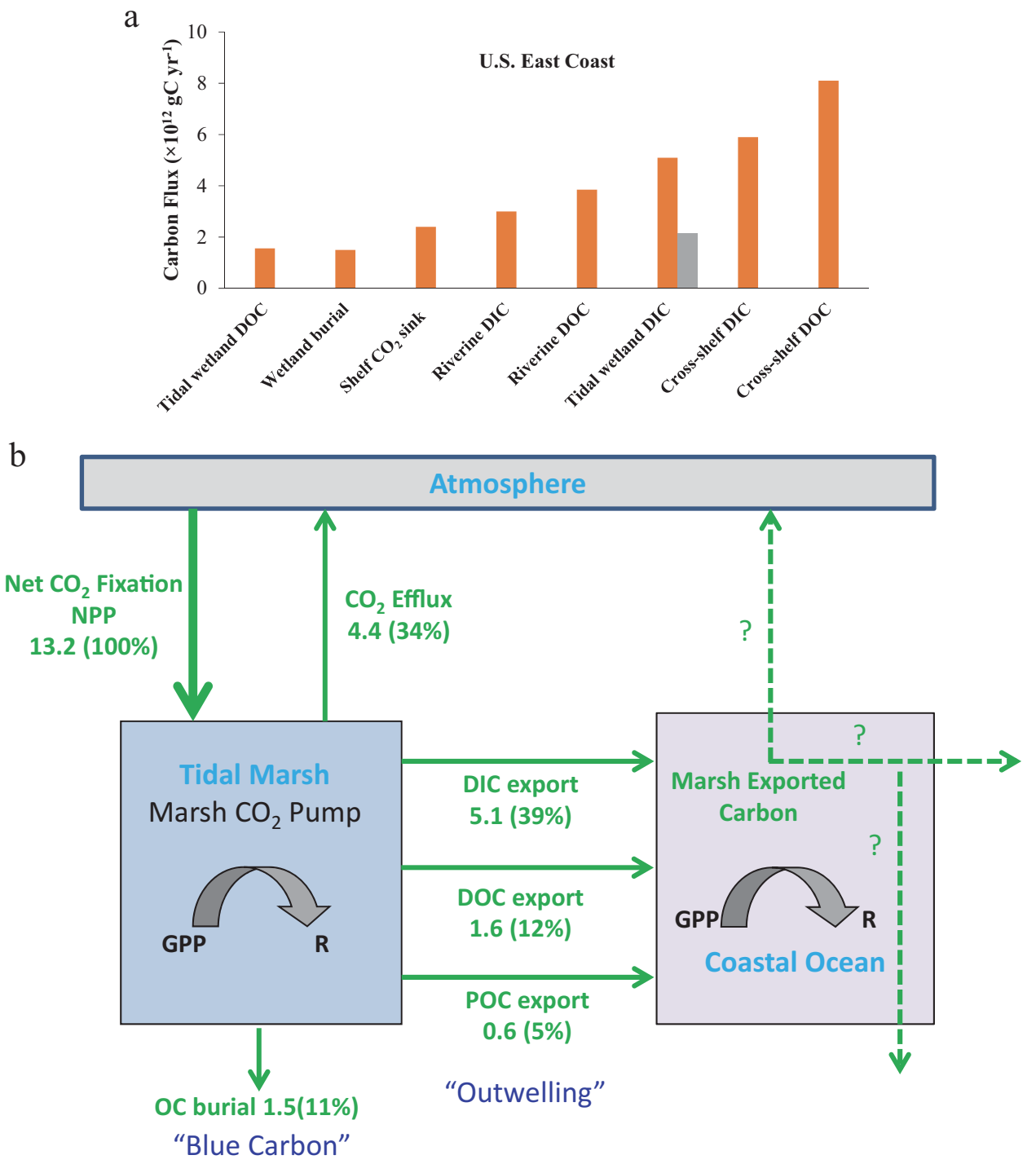

Fig. 7. Coastal carbon fluxes in the U.S. East (Atlantic) Coast. **(a)** Comparison of coastal carbon fluxes. Tidal wetland DIC flux was calculated using the annual areal DIC flux from this study and the total area of saline, brackish, and fresh water tidal marshes along the East Coast (9700 km^2 for saline and brackish marshes; 2600 km^2 for freshwater marshes). All other fluxes are adopted from (Najjar et al. 2012). The grey bar is mean tidal wetland DIC flux reported from the literature (Neubauer and Anderson 2003; Wang and Cai 2004; Cai 2011). **(b)** The tidal marsh carbon budget and the marsh CO_2 pump. Numbers are in Tg C yr^{-1}. The carbon fluxes are calculated by multiplying marsh areal carbon fluxes by the tidal wetland area of the East Coast (12,300 km^2), based on the Fish and Wildlife Service National Wetlands Inventory. Annual areal POC export is from Cai (2011); annual areal carbon burial and DOC export are from Kroeger et al. (2012). The areal CO_2 efflux from tidal water and marsh sediment is from Wang and Cai (2004) and Cai (2011); annual areal DIC export is from this study. Marsh NPP is the sum of all fluxes. GPP, gross primary production; R, total respiration.

hydrology likely affects DIC and DOC fluxes in a similar fashion. We therefore argue that it is expected that the DIC export is higher than the DOC export from marshes.

The sum of all carbon fluxes leaving marshes in Fig. 7b suggests that the total NPP of tidal marshes of the East Coast is about 13.2 Tg C yr^{-1} or 1071 g C m^{-2} yr^{-1}. This value agrees reasonably well with the mean value of ~1200 g C m^{-2} yr^{-1} based on synthesizing measured marsh NPP (Cai 2011; Hopkinson et al. 2012; Kroeger et al. 2012). Since we used a bottom-up method to estimate the NPP, such an agreement provides evidence that the new marsh DIC flux estimate is reasonable in balancing the marsh carbon budget.

"Marsh CO_2 pump" revisited

This study provides the first piece of direct evidence that DIC export fluxes from tidal marshes may be the primary fate for the CO_2 uptake by marsh plants, thus one of the largest terms in the marsh carbon budget and the coastal carbon cycle in the U.S. East Coast. Both changes in seawater carbonate chemistry following tidal exchange with the marsh and the magnitude of the DIC export from marshes provide clear evidence that tidal marshes are an important source of inorganic carbon to the coastal ocean and play an important role in modulating buffering capacity of coastal water over a long term. Thus, the diminishing extent of coastal wetlands in recent centuries and decades may have long-term implications to changes in water chemistry of the coastal ocean. If the current rapid rate of coastal wetland loss continues into the future, buffering capacity of coastal water might be gradually altered (Fig. 4). It is worth noting that all current knowledge of the coastal CO_2 systems is in a world with already diminished coastal wetland influence, such that currently there is no assessment of how seawater chemistry has changed in response to wetland loss.

In light of these new results, the "Marsh CO_2 Pump" concept (Wang and Cai 2004) can be further characterized: Tidal marshes behave as a strong CO_2 pump that takes up atmospheric CO_2 to grow marsh primary production; through the marsh internal carbon cycle, the majority of the NPP (>70%) is respired, and is either degassed to the atmosphere or exported as DIC to the coastal ocean (Fig. 7). A smaller portion (<20%) of the marsh NPP is also exported as DOC and POC. The rest of the marsh NPP (~10%) is likely buried as "blue carbon." Exports of DIC and alkalinity from tidal marshes are modulated mainly by aerobic and anaerobic respiration that can cause a decoupling between TA and DIC generation. These exports play an important role in regulating coastal water acid-base properties and buffering capacity. The seasonality of the Marsh CO_2 Pump corresponds to the growth-senescence cycle of marshes.

Collectively, tidal marshes may export more than 50% of their fixed CO_2 to the coastal ocean in the forms of organic and inorganic carbon (Fig. 7). The fate of marsh exported carbon is still unknown, but it ultimately determines how large the net marsh CO_2 sink really is. Since global continental shelves, including the U.S. East Coast, are a net sink of atmospheric CO_2 (Borges 2005; Cai 2011; Regnier et al. 2013; Signorini et al. 2013), it is reasonable to hypothesize that most of the carbon exported from marshes enters the internal carbon cycle on continental shelves (Fig. 7b, dash line arrows). Thereafter, part of the marsh exported carbon is hypothesized to be exported to open ocean as DOC and DIC. For the U.S. East Coast (Fig. 7a), marsh exported DIC alone could support a major portion of the cross-shelf export of DIC to the open ocean. It is possible that part of marsh exported carbon would be stored in marine sediments or in the deep ocean so that it is removed from the contemporary carbon cycle. Essentially, such a hypothesis supports that tidal marshes serve as an important atmospheric CO_2 sink, and is larger than the amount of carbon stored in marsh sediments alone (blue carbon). More studies are thus required to test these hypotheses and validate the "Marsh CO_2 Pump" concept. High-resolution measurements of both species concentrations and water fluxes are necessary to accurately define lateral transports from marshes to the coastal ocean. As demonstrated by this study, it is feasible to achieve such a goal with readily available sensors and careful modeling.

References

Bauer, J. E., W. J. Cai, P. A. Raymond, T. S. Bianchi, C. S. Hopkinson, and P. A. G. Regnier. 2013. The changing carbon cycle of the coastal ocean. Nature **504**: 61–70. doi:10.1038/nature12857

Borges, A. V. 2005. Do we have enough pieces of the jigsaw to integrate CO_2 fluxes in the coastal ocean? Estuaries **28**: 3–27. doi:10.1007/BF02732750

Bouillon, S., and others. 2008. Mangrove production and carbon sinks: A revision of global budget estimates. Global Biogeochem. Cycles **22**: GB2013, doi:10.1029/2007GB003052

Cai, W. J. 2011. Estuarine and coastal ocean carbon paradox: CO_2 sinks or sites of terrestrial carbon incineration? Ann. Rev. Mar. Sci. **3**: 123–145. doi:10.1146/annurev-marine-120709-142723

Cai, W. J., and Y. Wang. 1998. The chemistry, fluxes, and sources of carbon dioxide in the estuarine waters of the Satilla and Altamaha Rivers, Georgia. Limnol. Oceanogr. **43**: 657–668. doi:10.4319/lo.1998.43.4.0657

Capone, D. G., D. D. Reese, and R. P. Kiene. 1983. Effects of metals on methanogenesis, sulfate reduction, carbon-dioxide evolution, and microbial biomass in anoxic salt-marsh sediments. Appl. Environ. Microbiol. **45**: 1586–1591.

Chen, C. T. A., and A. V. Borges. 2009. Reconciling opposing views on carbon cycling in the coastal ocean: Continental shelves as sinks and near-shore ecosystems as sources of atmospheric CO_2. Deep-Sea Res. II **56**: 578–590. doi:10.1016/j.dsr2.2009.01.001

Childers, D. L., J. W. J. Day, and H. N. J. Mckellar. 2000. Twenty more years of marsh and estuarine flux studies:

Revisiting Nixon (1980), p. 391–423. In M. P. Weinstein and D. A. Kreeger [eds.], Concepts and controversies in tidal marsh ecology. Kluwer Academic.

Chmura, G. L., S. C. Anisfeld, D. R. Cahoon, and J. C. Lynch. 2003. Global carbon sequestration in tidal, saline wetland soils. Global Biogeochem. Cycles **17**. doi:1029/2002GB00191

Dickson, A. G., C. L. Sabine, and J. R. Christian. 2007. Guide to best practices for ocean CO_2 measurements. PICES Special Publication.

Downing, B. D., and others. 2009. Quantifying fluxes and characterizing compositional changes of dissolved organic matter in aquatic systems in situ using combined acoustic and optical measurements. Limnol. Oceanogr.: Methods **7**: 119–131. doi:10.4319/lom.2009.7.119

Duarte, C. M., J. J. Middelburg, and N. Caraco. 2005. Major role of marine vegetation on the oceanic carbon cycle. Biogeosciences **2**: 1–8. doi:10.5194/bg-2-1-2005

Egleston, E. S., C. L. Sabine, and F. M. M. Morel. 2010. Revelle revisited: Buffer factors that quantify the response of ocean chemistry to changes in DIC and alkalinity. Global Biogeochem. Cycles **24**. doi: 10.1029/2008GB003407

Friedrich, T., and A. Oschlies. 2009. Neural network-based estimates of North Atlantic surface pCO(2) from satellite data: A methodological study. J. Geophys. Res. Oceans **114**. doi: 10.1029/2007JC004646

Ganju, N. K. 2011. A novel approach for direct estimation of fresh groundwater discharge to an estuary. Geophys. Res. Lett. **38**. doi:10.1029/2011GL047718

Ganju, N. K., D. H. Schoellhamer, and B. A. Bergamaschi. 2005. Suspended sediment fluxes in a tidal wetland: Measurement, controlling factors, and error analysis. Estuaries **28**: 812–822. doi:10.1007/BF02696011

Ganju, N. K., M. Hayn, S. N. Chen, R. W. Howarth, P. J. Dickhudt, A. L. Aretxabaleta, and R. Marino. 2012. Tidal and groundwater fluxes to a shallow, microtidal estuary: Constraining inputs through field observations and hydrodynamic modeling. Estuaries Coast. **35**: 1285–1298. doi:10.1007/s12237-012-9515-x

Gedan, K. B., B. R. Silliman, and M. D. Bertness. 2009. Centuries of human-driven change in salt marsh ecosystems. Ann. Rev. Mar. Sci. **1**: 117–141. doi:10.1146/annurev.marine.010908.163930

Giblin, A. E. 1988. Pyrite formation in marshes during early diagenesis. Geomicrobiol. J. **6**: 77–97. doi:10.1080/01490458809377827

Giblin, A. E., and R. W. Howarth. 1984. Porewater evidence for a dynamic sedimentary iron cycle in salt marshes. Limnol. Oceanogr. **29**: 47–63. doi:10.4319/lo.1984.29.1.0047

Giblin, A. E., G. E. Likens, D. White, and R. W. Howarth. 1990. Sulfur storage and alkalinity generation in New-England Lake-sediments. Limnol. Oceanogr. **35**: 852–869. doi:10.4319/lo.1990.35.4.0852

Giblin, A. E., and R. K. Wieder. 1992. Sulfur cycling in marine and freshwater wetlands. *In* R. W. Howarth, J. W. Stewart, and M. V. Ivanov [eds.], Sulphur cycling on the Continents. SCOPE.

Hales, B., W. J. Cai, B. Mitchell, C. Sabine, and O. Schofield. 2008. North American continental margins: A synthesis and planning workshop, p. 3–13. *In* B. Hales, W. J. Cai, B. Mitchell, C. Sabine, and O. Schofield [eds.], Report of the North American Continental margins working group for the U.S. carbon cycle scientific group and interagency working group. U.S. Carbon Cycles Science Program.

Hales, B., and others. 2012. Satellite-based prediction of pCO(2) in coastal waters of the eastern North Pacific. Prog. Oceanogr. **103**: 1–15. doi:10.1016/j.pocean.2012.03.001

Herrmann, M., and others. 2015. Net ecosystem production and organic carbon balance of U.S. East Coast estuaries: A synthesis approach. Global Biogeochem. Cycles **29**: 96–111. doi:10.1002/2013GB004736

Hopkinson, C. S. 1988. Patterns of organic carbon exchange between coastal ecosystems—the mass balance approach in salt marsh ecosystems. *In* B.-O. Jansson [ed.], Coastal-offshore ecosystem interactions. Lecture notes on coastal and estuarine studies. Springer.

Hopkinson, C. S., and E. M. Smith. 2005. Estuarine respiration: An overview of benthic, pelagic, and whole system respiration, p. 122–147. In P. del Giorgio and P. Williams [eds.], Respiration in aquatic ecosystems. Oxford Univ. Press.

Hopkinson, C. S., W. J. Cai, and X. P. Hu. 2012. Carbon sequestration in wetland dominated coastal systems - a global sink of rapidly diminishing magnitude. Curr. Opin. Environ. Sustain. **4**: 186–194. doi:10.1016/j.cosust.2012.03.005

Howarth, R. W. 1979. Pyrite—its rapid formation in a salt-marsh and its importance in ecosystem metabolism. Science **203**: 49–51. doi:10.1126/science.203.4375.49

Howarth, R. W., and S. Merkel. 1984. Pyrite formation and the measurement of sulfate reduction in salt-marsh sediments. Limnol. Oceanogr. **29**: 598–608. doi:10.4319/lo.1984.29.3.0598

Hu, X. P., and W. J. Cai. 2011. An assessment of ocean margin anaerobic processes on oceanic alkalinity budget. Global Biogeochem. Cycles **25**. doi:10.1029/2010GB003859

Jiang, L. Q., W. J. Cai, and Y. C. Wang. 2008. A comparative study of carbon dioxide degassing in river- and marine-dominated estuaries. Limnol. Oceanogr. **53**: 2603–2615. doi:10.4319/lo.2008.53.6.2603

Kroeger, K. D., M. L. Cole, and I. Valiela. 2006. Groundwater-transported dissolved organic nitrogen exports from coastal watersheds. Limnol. Oceanogr. **51**: 2248–2261. doi:10.4319/lo.2006.51.5.2248

Kroeger, K., and others. 2012. Fluxes in tidal wetlands, p. 10–11. *In* R. G. Najjar, M.A.M. Friedrichs and W.-J. Cai [eds.], Report of the U.S. East Coast carbon cycle synthesis workshop.January 19-20, 2012. Ocean Carbon and Biogeochemistry Program and North American Carbon Program.

Kumar, M. D., M. D. George, and M. D. Rajagopal. 1993. Intertidal zones as carbon-dioxide sources to coastal oceans. Indian J. Mar. Sci. **22**: 221–224.

Lefevre, N., A. J. Watson, and A. R. Watson. 2005. A comparison of multiple regression and neural network techniques for mapping in situ pCO(2) data. Tellus B **57**: 375–384. doi:10.1111/j.1600-0889.2005.00164.x

Liu, K.-K., L. Atkinson, R. Quinones, and L. Talaue-McManus. 2010. Biogeochemistry of continental margins in a global context. *In* K.-K. Liu, L. Atkinson, R. Quinones, and L. Talaue-McManus [eds.], Carbon and nutrient fluxes in continental margins: A global synthesis. Springer.

MacCready, P. 2011. Calculating estuarine exchange flow using isohaline coordinates. J. Phys. Oceanogr. **41**: 1116–1124. doi:10.1175/2011JPO4517.1

Mackenzie, F. T., A. J. Andersson, A. Lerman, and L. M. Ver. 2004. Boundary exchanges in the global coastal margin: Implications for the organic and inorganic carbon cycles, p. 193–225. In A. R. Robinson and K. H. Brink [eds.], The sea. The global coastal ocean: Multiscale interdisciplinary processes. Harvard Univ. Press, Cambridge, MA.

Millero, F. J., T. B. Graham, F. Huang, H. Bustos-Serrano, and D. Pierrot. 2006. Dissociation constants of carbonic acid in seawater as a function of salinity and temperature. Mar. Chem. **100**: 80–94. doi:10.1016/j.marchem.2005.12.001

Morel, F. M. M., and J. G. Hering. 1993. Principles and applications of aquatic chemistry. John Wiley.

Morris, J. T., and G. J. Whiting. 1986. Emission of gaseous carbon-dioxide from salt-marsh sediments and its relation to other carbon losses. Estuaries **9**: 9–19. doi:10.2307/1352188

Najjar, R. G., M. Friedrichs, and W.-J. Cai. 2012. Report of the U.S. East coast carbon cycle synthesis workshop. January 19-20, 2012, Ocean Carbon and Biogeochemistry Program and North American Carbon Program, 34 pp.

Neubauer, S. C., and I. C. Anderson. 2003. Transport of dissolved inorganic carbon from a tidal freshwater marsh to the York River estuary. Limnol. Oceanogr. **48**: 299–307. doi:10.4319/lo.2003.48.1.0299

Odum, E. P. 1968. Energy flow in ecosystems—a historical review. Am. Zool. **8**: 11–18. doi:10.1093/icb/8.1.11

Pierrot, D., E. Lewis, and D. W. R. Wallace. 2006. MS Excel program developed for CO_2 system calculations. Carbon Dioxide Information Analysis Center, Oak Ridge National Laboratory.

Raymond, P. A., J. E. Bauer, and J. J. Cole. 2000. Atmospheric CO_2 evasion, dissolved inorganic carbon production, and net heterotrophy in the York River estuary. Limnol. Oceanogr. **45**: 1707–1717. doi:10.4319/lo.2000.45.8.1707

Raymond, P. A., and C. S. Hopkinson. 2003. Ecosystem modulation of dissolved carbon age in a temperate marsh-dominated estuary. Ecosystems **6**: 694–705. doi:10.1007/s10021-002-0213-6

Regnier, P., and others. 2013. Anthropogenic perturbation of the carbon fluxes from land to ocean. Nat. Geosci. **6**: 597–607. doi:10.1038/ngeo1830

Seitzinger, S. P., J. A. Harrison, E. Dumont, A. H. W. Beusen, and A. F. Bouwman. 2005. Sources and delivery of carbon, nitrogen, and phosphorus to the coastal zone: An overview of Global Nutrient Export fromWatersheds (NEWS) models and their application. Global Biogeochem. Cycles **19**. doi:10.1029/2005GB002606. doi:10.1029/2005GB002606

Signorini, S. R., and others. 2013. Surface ocean pCO(2) seasonality and sea-air CO_2 flux estimates for the North American east coast. J. Geophys. Res. Oceans **118**: 5439–5460. doi:10.1002/jgrc.20369

Smith, S. V., and J. T. Hollibaugh. 1993. Coastal Metabolism and the oceanic organic-carbon balance. Rev. Geophys. **31**: 75–89. doi:10.1029/92RG02584

Thomas, H., and others. 2009. Enhanced ocean carbon storage from anaerobic alkalinity generation in coastal sediments. Biogeosciences **6**: 267–274. doi:10.5194/bg-6-267-2009

Wagner, R. J., R. W. J. Boulger, C. J. Oblinger, and B. A. Smith. 2006. Guidelines and standard procedures for continuous water-quality monitors—station operation, record computation, and data reporting, p. 51.

Wang, Z. A., and W. J. Cai. 2004. Carbon dioxide degassing and inorganic carbon export from a marsh-dominated estuary (the Duplin River): A marsh CO_2 pump. Limnol. Oceanogr. **49**: 341–354. doi:10.4319/lo.2004.49.2.0341

Wang, Z. A., R. Wanninkhof, W. J. Cai, R. H. Byrne, X. P. Hu, T. H. Peng, and W. J. Huang. 2013. The marine inorganic carbon system along the Gulf of Mexico and Atlantic coasts of the United States: Insights from a transregional coastal carbon study. Limnol. Oceanogr. **58**: 325–342. doi:10.4319/lo.2013.58.1.0325

Warner, J. C., B. Armstrong, R. Y. He, and J. B. Zambon. 2010. Development of a Coupled Ocean-Atmosphere-Wave-Sediment Transport (COAWST) modeling system. Ocean Model. Online **35**: 230–244. doi:10.1016/j.ocemod.2010.07.010

Acknowledgments

We thank Adrian Mann, Katherine Hoering, Sandra Brosnahan, Linda Kraemer, Thomas Kraemer, T. Wallace Brooks, Julia Signell, Jennifer O'keefe Suttles, Alterra Sanchez, Michael Casso, John Pohlman, Jordan Mora, Patrick Dickhudt, Yue Qiu, and the staff of Waquoit Bay NERR for sampling, logistical, and analysis support. All data and models presented in the paper can be obtained from Zhaohui Aleck Wang (zawang@whoi.edu) upon request. The study is funded by the USGS Coastal & Marine Geology Program, U.S. National Science Foundation (OCE-1459521), NOAA Science Collaborative (NA09NOS4190153), and USGS LandCarbon Program. Any use of trade, firm or product names is for descriptive purposes only and does not imply endorsement by the U.S. Government.

Submitted 23 December 2015
Revised 15 April 2016
Accepted 28 April 2016

Associate editor: M. Dileep Kumar